

Effects of laser bandwidth on Iso-Dense Bias and Line End Shortening at sub-micron process nodes

R. C. Peng*, A. K. Yang, L. J. Chen, Y. W. Guo, H. H. Liu, John Lin,
TSMC Corp., Hsinchu Science Park, Hsinchu, Taiwan 300-77, R.O.C
Allen Chang,
Cymer Inc., Kuang Fu Rd. Hsinchu, Taiwan, R.O.C

ABSTRACT

Control of Isolated and Dense line Bias (IDB) and Line End Shortening (LES) in a lithographic process has become increasingly important, particularly for the 65nm node and below. The IDB depends on many factors, for example, focus, lens aberrations, partial coherence and laser spectral bandwidth. This work studies the impact to IDB and LES from changes in laser bandwidth at two sub-micron process nodes. Careful measurements of both FWHM and E95 bandwidth parameters of the laser spectral profile were carried out using two types of spectrometers. The spectral bandwidth was adjusted over a larger range than normally experienced during wafer exposures by carefully varying the laser operating conditions to provide controlled changes in bandwidth while maintaining all other laser performance parameters within specification. Measurements of both linewidth and LES on several substrates were made and correlated with laser bandwidth to determine the sensitivity of IDB and LES to bandwidth variation. The sensitivity of different structures to E95 bandwidth variation was assessed

Keywords: Optical Proximity Effect, Iso-Dense Bias, Line End Shortening, Laser, Bandwidth, E95

INTRODUCTION

According to the 2005 lithography roadmap of the International Technology Roadmap for Semiconductors (ITRS), shown in Table 1, CD control is quite a challenge since these requirements must be met through-pitch, intra-die, and die-to-die. One of the keys for CD control is correction of Optical Proximity Effects (OPE). For IC makers, it has become increasingly challenging to process various products at sub-micron nodes with stable and controllable OPE performance. To control OPE, tool parameters such as illumination partial coherence, lens numerical aperture, laser bandwidth and focus need to be well controlled, in addition to control of process parameters and pattern layout. Laser bandwidth is one of the critical factors. Variations in laser bandwidth will cause defocus errors because of chromatic aberration in the projection lens, resulting in contrast loss and hence changes in OPE.

Year of Production	2007	2010	2013	2016
DRAM and Flash				
DRAM 1/2 Pitch (nm) (contacted)	65	45	32	22
Flash 1/2 Pitch (nm) (Un-contacted Poly)	57	40	28	20
CD control (3 sigma) (nm)	6.6	4.7	3.3	3.0
MPU				
MPU/ASIC Metal 1 (M1) 1/2 Pitch (nm) (contact)	68	45	32	23
Gate CD control (3 sigma) (nm)	2.6	1.9	1.3	0.9

Table-1 Lithography roadmap of International Technology Roadmap for Semiconductors (ITRS), 2005

Experimental and simulation work on the effects of laser bandwidth has been carried out in the past [1][2][3]. The bandwidth metrics, Full Width at Half Maximum (FWHM) and E95, have been clearly defined. One-dimensional optical proximity performance and CD sensitivity to laser bandwidth changes for a 80nm technology node process were also recently reported [3]. The effect of laser bandwidth at more advanced process nodes is unknown. This paper will provide Iso-Dense Bias (IDB) and Line End Shortening (LES) results, which show the one-dimensional and two-dimensional optical proximity performance at two sub-micron process nodes under evaluation. Additionally, the capability of on-board laser bandwidth metrology (for both FWHM and E95) will be assessed by comparison to a precise external reference spectrometer.

LASER BANDWIDTH CONTROL AND EXPERIMENTAL CONDITIONS

2.1 Laser bandwidth control

Excimer lasers typically operate using a combination of an inert gas (argon, krypton, or xenon) and a reactive gas (fluorine or chlorine). For example, Argon-Fluorine excimers give stimulated emission at around 193nm wavelength and this can be line-narrowed for use in wafer microlithography patterning tools. During wafer exposures, the laser produces a well-controlled wavelength and bursts of pulses under control of the wafer scanner. The spectrum for the accumulation of pulses in the burst is a convolution of the spectra of the individual pulses and the pulse-to-pulse wavelength variation. This spectrum is the relevant laser bandwidth which determines imaging performance. To quantify laser bandwidth, we use the metrics of FWHM and E95, which were clearly defined by Kroyan [2]. As the optical proximity requirements for advanced process nodes becomes more stringent than before, control of FWHM and E95 is more critical, especially E95, which has been shown to correlate well with optical proximity effects [2].

Measuring laser bandwidth was not easy several years ago because the instrumentation was not yet capable of high accuracy measurements. Now, Cymer has developed an on-board metrology unit, called the Bandwidth Analysis Module (BAM). By illuminating an etalon to produce a fringe pattern that is monitored using a photodiode array and corrected for a number of systematic errors, both E95 and FWHM can be derived by sophisticated modeling of the etalon fringe pattern. Using the BAM, both FWHM and E95 performance may be monitored to better than 0.01pm precision. The on-board BAM metrology was standard on the exposure tool used for the more advanced process node under evaluation in this work.

In this study, the illumination source is a Cymer XLA series laser, which is dual chamber MOPA design with a Master Oscillator (MO) and Power Amplifier (PA). To change the bandwidth, we can adjust the fluorine concentration of the MO and/or control the delay time between the firing of the MO and PA chambers. The relationship between fluorine concentration, differential timing and E95 bandwidth has been presented previously [4]. By using this methodology to obtain the curves of fluorine concentration and differential timing for various E95 settings, we can pick suitable settings for the experiment, including the corresponding FWHM bandwidth. Three bandwidth settings at each of two technology nodes were used in this experiment, as shown in Table-2.

	Node-A		Node-B	
	E95	FWHM	E95	FWHM
Setting-1	0.36	0.16	0.30	0.14
Setting-2	0.47	0.19	0.40	0.16
Setting-3	0.62	0.22	0.52	0.20

Table-2 Laser bandwidth setting

2.2 Lithography experimental condition

To characterize optical proximity performance, we used the test layout of Figure-1 to check IDB and LES. The layout includes a vertical line and a number of horizontal lines. The central line is the reference for CD. The gap between the vertical line and horizontal lines is called Gap1 (End-Line). The gap between two horizontal lines is

called Gap2 (End-End). This is a common layout. The measurement locations are the CD of the central line, Gap1 and Gap2. LES is evaluated separately for both Gap 1 and Gap 2. The definition of IDB is as follows:

$$IDB = CD_{\text{iso line}} - CD_{\text{dense line}}$$

Where $CD_{\text{iso line}}$ is the feature size of the isolated line

$CD_{\text{dense line}}$ is the feature size of the dense line

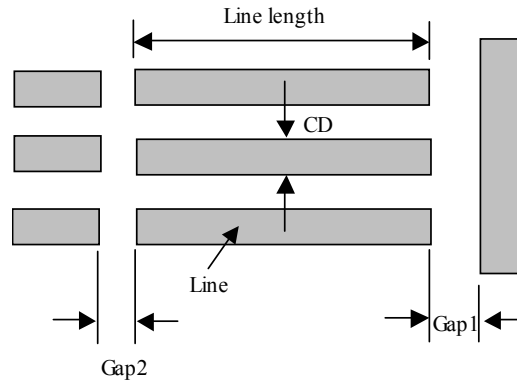


Figure-1 Test layout: the drawing and definition of the measured points

According to the definition of IDB, the dense line CD is the reference because it is less sensitive than the isolated line CD to changes in focus (or bandwidth). For LES, we take the difference between the measured and the target CDs of Gap1 and Gap2. Simulations of these structures, for comparison to experiment, were also carried out using Prolith version 9.3.3 with full, high resolution laser spectral input.

The lithography experimental conditions are listed in Table-3. Both process technology nodes were exposed with ASML scanners and Cymer Lasers. Both nodes used Attenuated Phase Shift Masks. NA is larger than 0.70 for Node-A and larger than 0.9 for Node-B. We pick the minimum pitch as the dense line and the most isolated line as the isolated line for both nodes. For CD measurements, we used a Scanning Electron Microscope (SEM) to measure lines and gaps. Scanner and laser parameters were recorded and controlled within specifications during all bandwidth adjustments to reduce experimental noise.

	Node-A	Node-B
Scanner	ASML scanner	ASML scanner
Laser	Cymer XLA-100	Cymer XLA-300
Mask	APSM	APSM
NA	>0.70	>0.90
Pitch	Dense line: minimum pitch of node-A Iso line: most isolated line in node-A	Dense line: minimum pitch of node-B Iso line: most isolated line in node-B
Metrology	SEM	SEM

Table-3 Experimental conditions including scanner, laser, mask, NA, pitch and metrology

EXPERIMENTAL RESULTS

3.1 OPE and IDB performance

Linewidth was measured at seven pitches between dense (1:1) and isolated. The results for both Node A and Node B are shown in Figure-2.

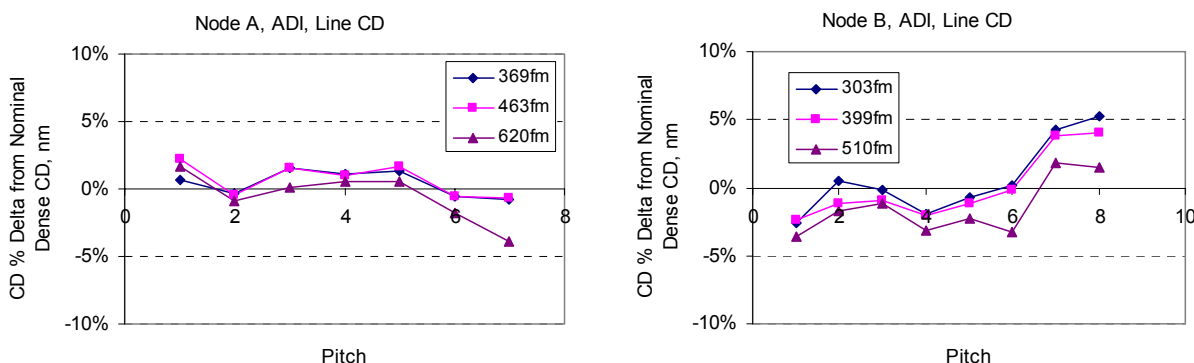


Figure-2: CD % deviation from nominal dense CD through pitch for (a) Node A and (b) Node B

The OPE curves are shown at the three bandwidths measured, the lowest bandwidth being closest to the nominal imaging conditions. The lowest two bandwidth conditions showed little difference in the shape of the curve. Slight deviations were apparent for the highest bandwidth case, although the CD error was less than 5% in all cases. This change in the shape of the OPE curve resulted in an increase in the range of CD variation for Node A, although it resulted in a decrease in the CD range for Node B. This was likely due to a slightly different exposure bias condition between the two cases. As expected, the change in CD was larger for more isolated features, which are well known to be more sensitive to changes in contrast.

IDB, the difference between the CD of dense lines and isolated lines is often used to characterize optical proximity performance. We evaluated the IDB for both nodes at the various bandwidth conditions listed in Table-2. The results are compared to simulations in Figure-3. The BAM E95 reading is shown on the x-axis and the IDB CD change is shown on the y-axis. The simulated data is shown as diamonds and the measured data is shown as squares. These results are for CD measured after resist develop and before the etching step. In these charts, we take CD at E95=0.36 μ m as the reference bandwidth for Node A, and E95=0.30 μ m as the reference bandwidth for Node B, and show CD change as the difference between the reference CD and the measured CD at the other bandwidth conditions. Both nodes show excellent agreement between simulation and experiment. For Node-A, the CD sensitivity to bandwidth, by simulation is ~ 0.8 nm per 0.1 μ m E95 change. In the actual measured data, the CD sensitivity to E95 is ~ 1.1 nm per 0.1 μ m E95 change. For Node B, the CD sensitivity to E95 bandwidth is ~ 0.7 nm per 0.1 μ m E95 change for the simulations and ~ 0.8 nm per 0.1 μ m E95 change for the measured data.

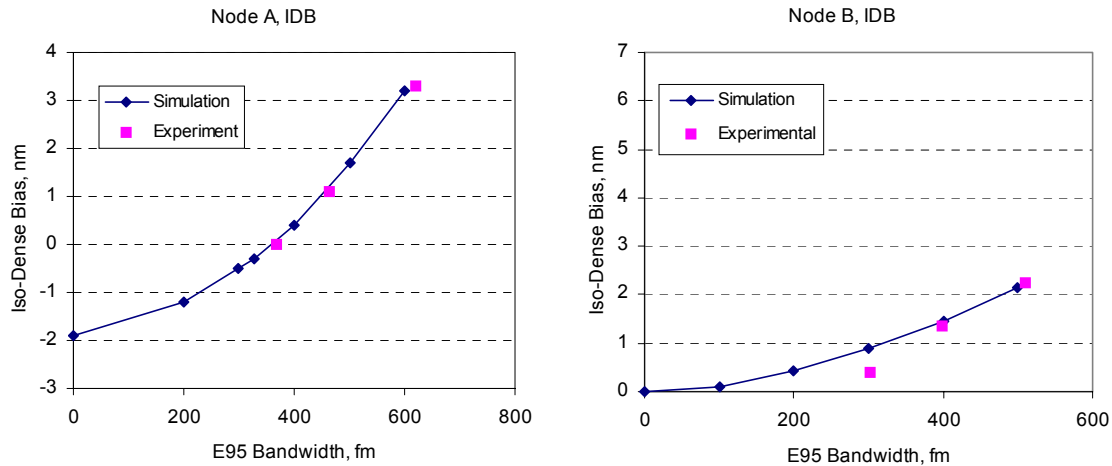


Figure-3. Simulated and experimental IDB for (a) Node A and (b) Node B as a function of E95 bandwidth. It is interesting that the sensitivity to bandwidth is lower for the more advanced process node. A clue as to whether this might be expected may be gained from examining the isolated line CD-focus curves for the two processes. The response of these lines to changes in contrast (defocus) gives a good indication of the response to changing bandwidth, and will be the dominant factor in determining IDB since dense lines are relatively insensitive to changes in contrast. These CD-focus curves are shown in Figure-4. It can be seen that the Depth of Focus (DOF) for Node B lines is actually slightly greater than that for Node A, and suggests that the lower bandwidth sensitivity observed may indeed be a consequence of the optimized process conditions for this node.

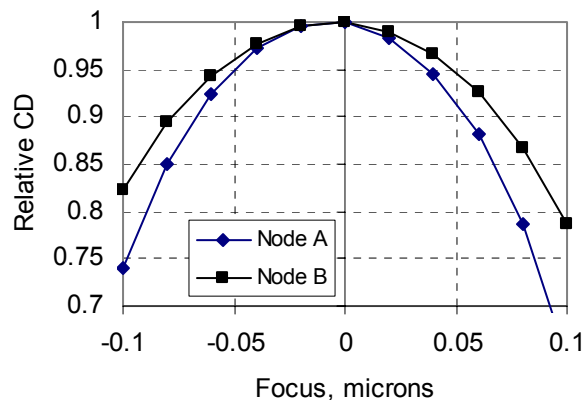


Figure-4. CD-focus response for Node A and Node B isolated lines

3.2 Line End Shortening (LES) performance

LES, the shrinkage of line length, for the various bandwidth conditions listed in Table-2 is shown in Figure-5 for the seven pitches used previously. The measurement data for Gap 1 (End-Line pullback) is suspicious since it indicates a smaller gap than the design dimension and is almost insensitive to the bandwidth condition. When reviewing the SEM pictures for the measured lines, we found significant resist residue remaining at the end of the line, particularly for the highest bandwidth conditions, as shown in Figure-6. The decrease in the gap dimension was more noticeable for the End-Line case because the pullback in this case is less than the End-End case. This residue was also observed for wafers printed at Node B.

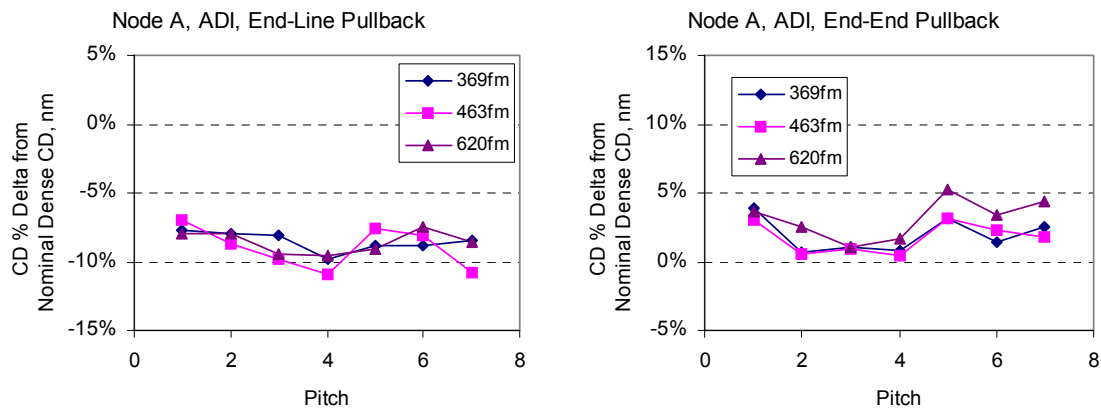


Figure-5. LES for Node A for (a) End-Line (Gap 1) and (b) End-End (Gap 2)

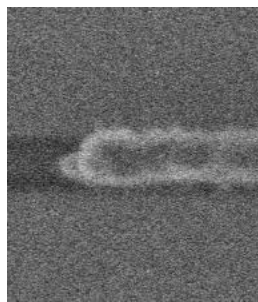


Figure-6 Residue at the end of line in the worse bandwidth condition

To improve the accuracy of the LES measurements, we etched the wafers to see if we could remove the residue. We checked the profile at the end of the line after etch and found that the residue had been removed. Unfortunately, only the Node-A wafers could be etched so no LES data is available for the Node-B case.

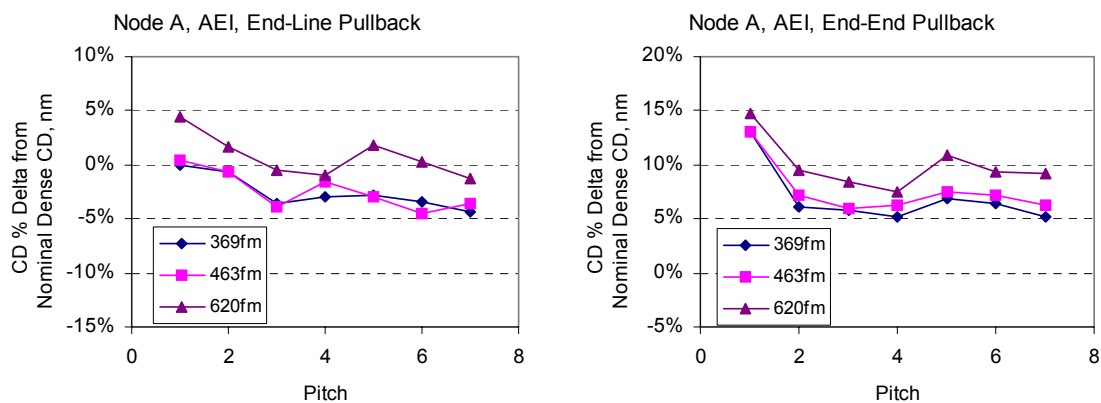


Figure-7. After-etch LES measurements of Node A for (a) End-Line and (b) End-End

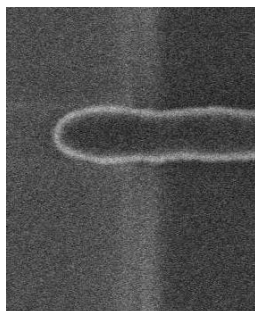


Figure-8 The end of line after the etching stage in the worst bandwidth condition

Figure-7 shows the results of LES measurements on Node-A wafers after the etching stage. The trend of measured data is now more consistent with the trends observed in the IDB data. Dense lines showed greater line end pullback at all bandwidths and the effect of increasing bandwidth was consistent across the range of pitches. Figure-8 is the picture of line after the etching stage and it shows the residual is removed. The sensitivity to bandwidth for LES (averaged through pitch) was compared to simulation and is shown in Figure-9. Agreement between measurement and simulation was good. For End-Line pullback, simulation showed $\sim 1.6\text{nm}/0.1\text{pm}$ and experiment showed $\sim 1.7\text{nm}/0.1\text{pm}$. For End-End line pullback, simulation showed $\sim 2.4\text{nm}/0.1\text{pm}$ and the measured results showed $\sim 2.9\text{nm}/0.1\text{pm}$ (after correction for the pullback due to two line ends). As expected, the End-End case showed greater pullback and greater sensitivity to bandwidth. Also, as expected, these levels of sensitivity are greater than those observed for linewidth CD due to the 2-D contrast loss effects at the line ends. Fortunately, correction of pullback using hammerheads, serifs etc should significantly reduce this sensitivity and this is the subject of ongoing work.

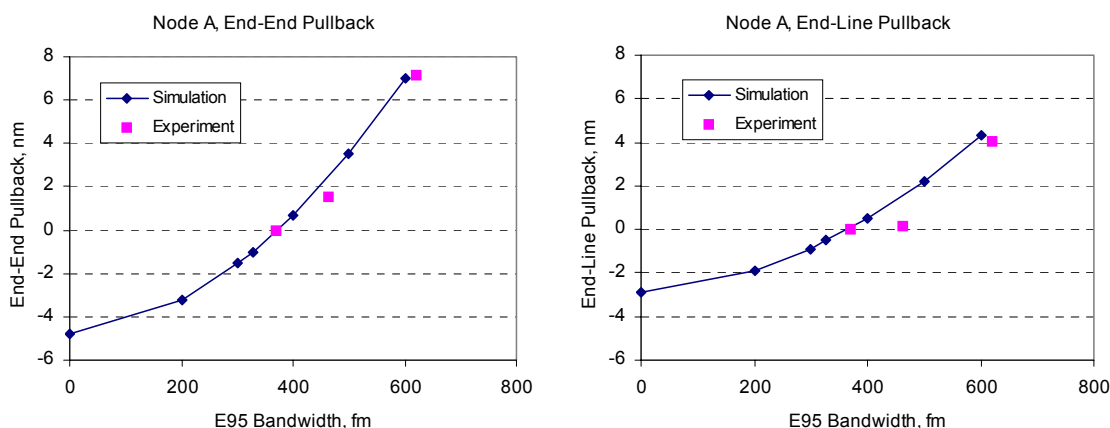


Figure-9. Comparison of simulation and experiment for LES for Node A for (a) End-Line and (b) End-End

DISCUSSION AND CONCLUSIONS

In this paper, we checked the OPE, IDB and LES sensitivity to laser bandwidth for two sub-micron process nodes. A summary of the CD sensitivity results is shown in Table-4. Based on these results, it appears that the experimentally observed behavior is matched quite well to simulation results. In the case of LES, it is important to remove experimental noise due to resist residue by etching the wafers.

Although the CD changes due to bandwidth were small, typically less than 1nm, the CD budgets at these advanced process nodes are shrinking rapidly and we must ensure that this contribution does not become a significant part of the total budget. This study presents some of the first experimental work on the effects of bandwidth on two-dimensional structures. As expected, the sensitivity to bandwidth of line length is greater than that of linewidth. While OPC may be easier to implement in these regions, this is an area that needs further investigation to ensure that it does not impact overlay and device performance.

There is some evidence from this work, and previous work, that bandwidth sensitivity can be reduced by carefully optimizing process conditions. The other key factor is that laser suppliers must continually strive to reduce bandwidth fluctuations during wafer processing. Both passive and active methods for controlling bandwidth continue to be developed to improve this area of performance.

CD Sensitivity(per 0.1pm E95 BW change)	Iso-Dense Bias		Line End Shortening			
			End-Line		End-End	
	Simulation	Experiment	Simulation	Experiment	Simulation	Experiment
Node A	0.8	1.1	1.6	1.7	2.4	2.9
Node B	0.7	0.9	-	-	-	-

Table-4. Summary of IDB and LES sensitivity to bandwidth

ACKNOWLEDGEMENTS

Thanks to Joe Bendik at Dynamic Intelligence Inc. for the simulation work.

REFERENCES

- [1] Armen Kroyan, Nigel Farrar, Joseph Bendik, Olivier Semprez, Chris Rowan Chris A. Mack “Modeling the Effects of Excimer Laser Bandwidths on Lithographic Performance” Proc. SPIE Vol.4000, 658(2000)
- [2] Armen Kroyan, Ivan Lalovic, Nigel Farrar “Effects of 95% Integral vs. FWHM Bandwidth Specifications on Lithographic Imaging” Proc. SPIE 4346, 1244 (2001)
- [3] Kevin Huggins, Toki Tsuyoshi, Meng Ong, Robert Rafac, Christopher Treadway, Devashish Choudhary, Takehito Kudo, Shigeru Hirukawa, Stephen P. Renwick, and Nigel R. Farrar “Effects of Laser Bandwidth on OPE in a modern lithography tool” Proc. SPIE 6154, 61540Z (2006)
- [4] Wayne J. Dunstan, Robert Jacques, Robert J. Rafac, Rajasekhar Rao and Fedor Trintchouk “Active Spectral Control of DUV Light Source for OPE Minimization” Proc. SPIE 6154, 61542J (2006)